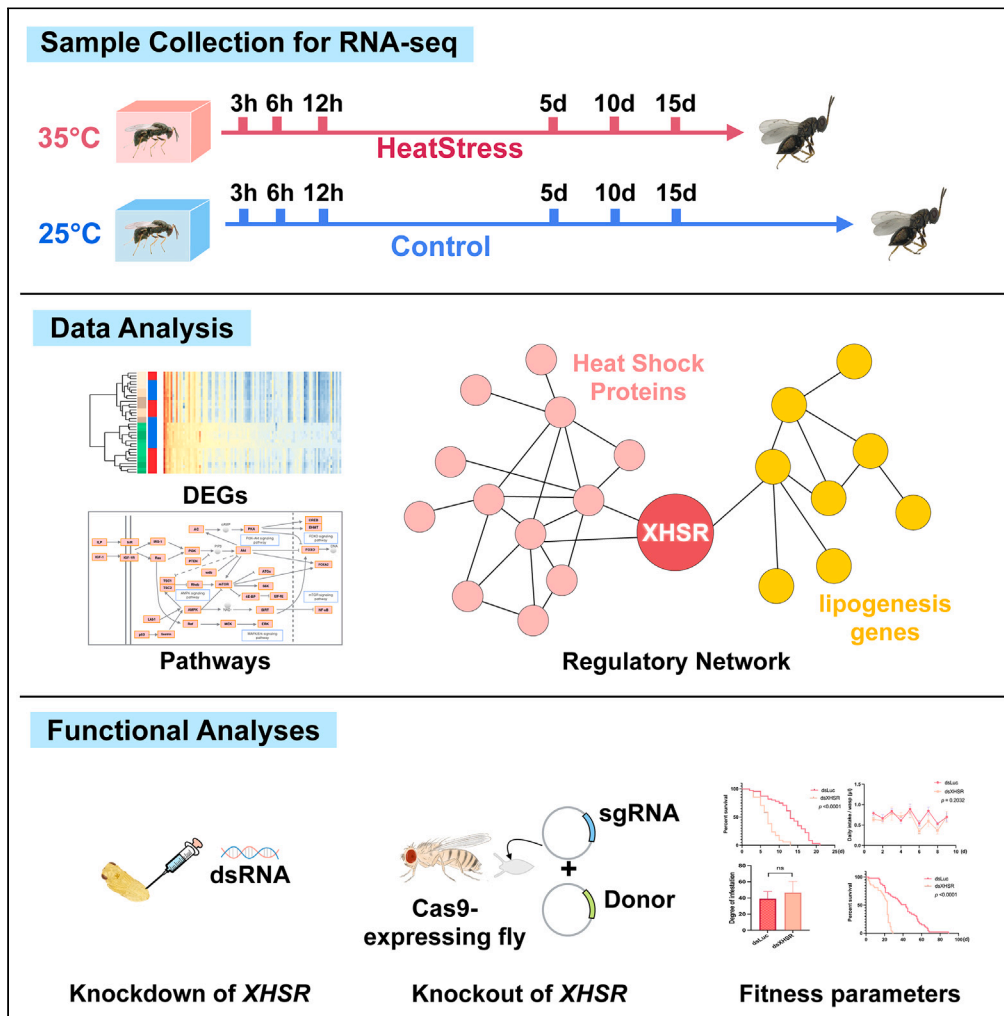


Article

Regulatory network in heat stress response in parasitoid wasp focusing on *Xap5* heat stress regulator



Shijiao Xiong, Kaili Yu, Haiwei Lin, ..., Qisheng Song, Qi Fang, Gongyin Ye

fangqi@zju.edu.cn

Highlights

Constructed a regulatory network for heat stress responses

Identified *XHSR* as a key regulator, validated via knockdown experiments

Confirmed *XHSR*'s role in heat stress via CRISPR/Cas9 knockout in *Drosophila*

Xiong et al., iScience 27, 108622  
January 19, 2024 © 2023 The Authors.  
<https://doi.org/10.1016/j.isci.2023.108622>



## Article

Regulatory network in heat stress response in parasitoid wasp focusing on *Xap5* heat stress regulator

Shijiao Xiong,<sup>1</sup> Kaili Yu,<sup>1</sup> Haiwei Lin,<sup>1</sup> Xinhai Ye,<sup>1</sup> Shan Xiao,<sup>1</sup> Yi Yang,<sup>1</sup> David W. Stanley,<sup>2</sup> Qisheng Song,<sup>3</sup> Qi Fang,<sup>1,4,\*</sup> and Gongyin Ye<sup>1</sup>

## SUMMARY

**Insects are susceptible to elevated temperatures, resulting in impaired fertility, and shortened lifespan. This study investigated the genetic mechanisms underlying heat stress effects. We conducted RNA sequencing on *Pteromalus puparum* exposed to 25°C and 35°C, revealing transcriptional signatures. Weighted Gene Co-expression Network Analysis uncovered heat stress-associated modules, forming a regulatory network of 113 genes. The network is naturally divided into two subgroups, one linked to acute heat stress, including heat shock proteins (HSPs), and the other to chronic heat stress, involving lipogenesis genes. We identified an *Xap5* Heat Shock Regulator (*XHSR*) gene as a crucial network component, validated through RNA interference and quantitative PCR assays. *XHSR* knockdown reduced wasps' lifespan while directly inducing HSPs and mediating lipogenesis gene induction. CRISPR/Cas9-mediated knockout of the *Drosophila* *XHSR* homolog reduced mutants' survival, highlighting its conserved role. This research sheds light on thermal tolerance mechanisms, offering potential applications in pest control amid global warming.**

## INTRODUCTION

Global warming poses a significant threat to terrestrial, aquatic, and marine ecosystems. The increased temperatures can lead to severe impacts on water availability and agricultural production, resulting in steep declines in total food production, some of which may appear as early as 2040.<sup>1</sup> The warming also leads to the extinction and migration of key species, which causes serious changes in community structures.<sup>2–4</sup> Insects are particularly vulnerable to the impacts of global warming, because their complex physiological systems are heavily impacted by climate.<sup>5,6</sup> These negative impacts translate into reduced abilities to carry out essential life functions, such as foraging, mate-finding, mating, and producing viable progeny. Generally, parasitoid wasps are more susceptible to thermal stress than their hosts.<sup>7</sup> As the most diverse group of insects, parasitoid represent a tremendous potential for biological control of insect pests.<sup>8</sup> They are reared, transported among many countries, and applied in many cropping systems. They provide agricultural benefits at the levels of food security and environmental stewardship because they contribute to reducing the broadcast use of chemical insecticides. *Pteromalus puparum* is a cosmopolitan parasitoid wasp that uses numerous pest species as hosts, including the pupal stage of the butterfly *Pieris rapae*.<sup>9</sup> Field surveys documented high rates of parasitism by *P. rapae* in East China, with up to 90% during early summer and 59–62% during winter.<sup>10</sup> However, elevated environmental temperatures exert serious negative influence on *P. puparum*, recorded as reduced developmental rates, altered sex ratios, and reduced offspring density per host pupa. These data document diminished potential for pest population control.<sup>11</sup>

Elevated environmental temperatures do not influence parasitoid species and other insect species in a uniform manner. The aphid *Sitobion avenae* demonstrated increased heat tolerance and longevity in response to higher temperatures.<sup>12</sup> Alternatively, the adult lifespan of the true bug, *Diaphorina citri*, was reduced by 74% at 41°C.<sup>13</sup> Such variations may, in some species, be related to durations of heat exposure, as well as genetic and ecological factors. Insects employ a variety of genetic responses to cope with heat stress, including the regulation of HSPs, antioxidant enzymes, and lipid metabolism-related genes.<sup>14–16</sup> The crucial role of HSPs in insects' responses to heat stress is frequently emphasized, as they function as stress proteins or molecular chaperones.<sup>17,18</sup> Transcriptome analyses indicate that the expression of genes encoding heat shock protein 70 (HSP70) acts to prolong the lifespan of *Drosophila melanogaster* under short-term heat stress.<sup>19</sup> However, longer exposures to severe heat stress inhibited HSP expression and activated the expression of genes that lead to apoptosis, causing irreversible tissue damage.<sup>20,21</sup> Another study showed that repeated episodes of mild heat stress in female *Drosophila* increased their resistance

<sup>1</sup>State Key Laboratory of Rice Biology and Breeding & Ministry of Agricultural and Rural Affairs Key Laboratory of Molecular Biology of Crop Pathogens and Insects, Institute of Insect Sciences, Zhejiang University, Hangzhou 310058, China

<sup>2</sup>USDA/ARS Biological Control of Insects Research Laboratory, 1503 S. Providence Road, Columbia MO, USA

<sup>3</sup>Division of Plant Sciences, University of Missouri, Columbia, MO, USA

<sup>4</sup>Lead contact

\*Correspondence: [fangqi@zju.edu.cn](mailto:fangqi@zju.edu.cn)

<https://doi.org/10.1016/j.isci.2023.108622>



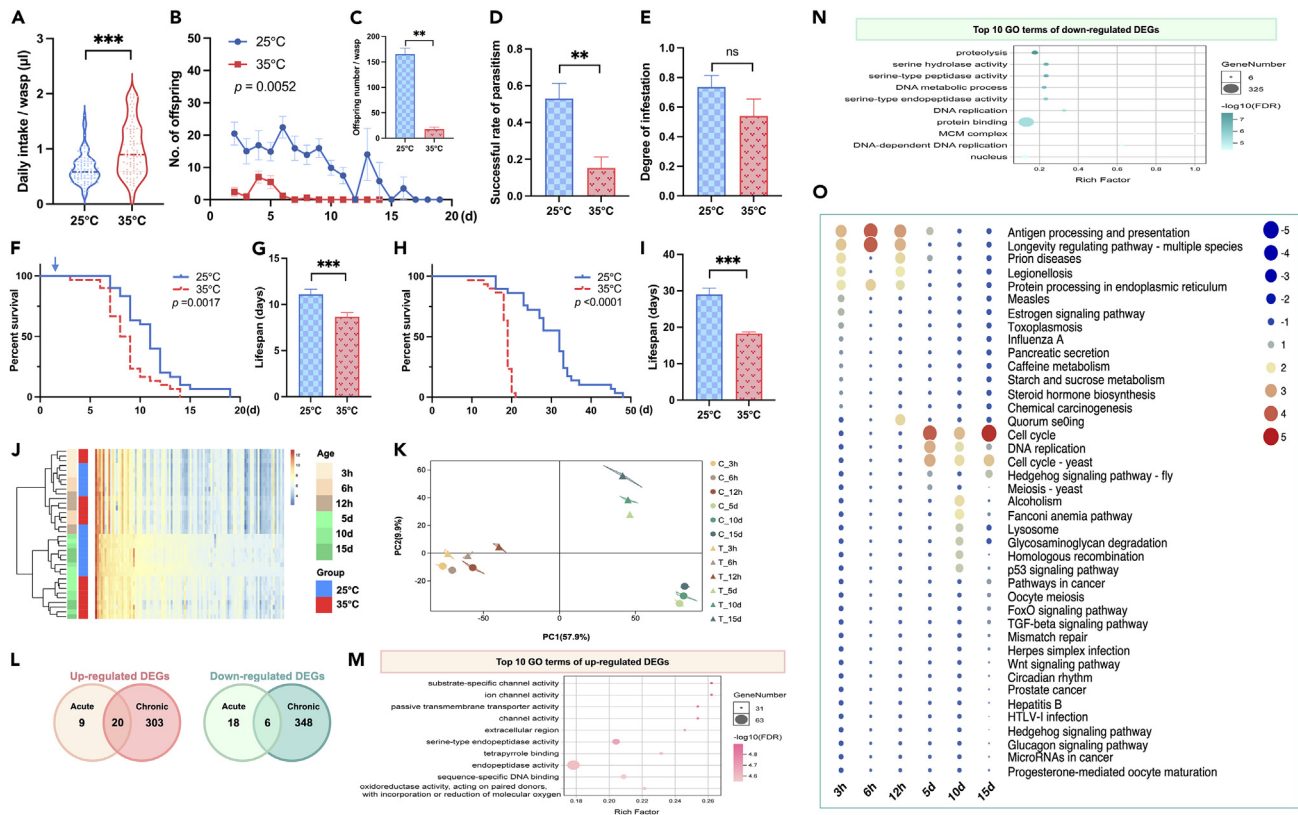


**Figure 1. The effects of heat stress on fitness parameters and gene expression in *Pteromalus puparum***

Means  $\pm$  SEM. \*\* means  $p < 0.01$ , \*\*\* means  $p < 0.0001$ , ns means  $p > 0.05$ .

(A) Daily food intake per wasp during the adult stage from eclosion to death, under 25°C and 35°C. The dotted line indicated median intake; (B) Daily number of offspring each female wasp produced from two days after eclosion to death, under 25°C and 35°C; (C) Total offspring number per female wasp produced throughout its adult stage, under 25°C and 35°C; (D) Successful rate of parasitism by wasps under 25°C and 35°C; (E) Degree of infestation by wasps under 25°C and 35°C; (F) Survival of adult female wasps under 25°C and 35°C, with hosts provided from two days after eclosion; (G) Lifespan of adult female wasps under 25°C and 35°C, with hosts provided from two days after eclosion; (H) Survival of adult female wasps during adult stage from eclosion to death under 25°C and 35°C. Wasps had never mated or oviposited. (I) Lifespan of adult female wasps during adult stage from eclosion to death under 25°C and 35°C. (J) Heatmap and cluster analysis. Each row includes 100 genes from a transcriptome sample selected using a random function, and the grouping information is labeled as "Age" and "Group" on the right side of the graph. Brown blocks from light to dark indicate 3 h, 6 h and 12 h, while green blocks from light to dark indicate 5 days, 10 days and 15 days, respectively. The blue blocks indicate the 25°C group, labeled "25°C," and the red blocks indicate the 35°C group, labeled "35°C." Each column represents one gene. Each cell represents the expression of a gene in a sample, expressed as log<sub>2</sub>(FPKM+1), from 0 to 14 corresponding to the color from blue to red; (K) Graphs show the first two principal components (PC) explaining gene expression levels in all female wasps. Each data point represents a biological replicate, with PC coordinates determined using regularized log transformed read counts; (L) Venn diagram depicting the definition of genes altered by mild heat stress. DEGs are classified as genes responding to acute and chronic heat stress and are displayed according to up- or down-regulation of gene expression; (M) Top 10 GO terms of GO enrichment of up-regulated DEGs; (N) Top 10 GO terms of GO enrichment of down-regulated DEGs; (O) Results of the KEGG pathway enrichment analysis of DEGs, with circles indicating the number of DEGs significantly enriched to this pathway.

to acute heat stress via a decrease in dopamine level,<sup>22</sup> contributing to the regulation of energy and lipid metabolism.<sup>23</sup> Despite these findings, the overall pattern of insect responses and potential mechanisms for elevated environmental temperatures remain unclear.<sup>16</sup>

Based on the significance of parasitoid wasps in agriculture, meaningful clarity on how specific parasitoids respond to environmental temperatures and the range of survivable environmental changes these insects can withstand is necessary. In this study, we examined the genetic regulatory network and the function of hub genes involved in the effects of heat stress on the fitness traits of *P. puparum*.

## RESULTS

### Heat stress induces distinct genetic network responses

The biological fitness parameters of *Pteromalus puparum* undergo significant changes as the environmental temperature rises. After adult wasps were subjected to heat stress (35°C), their daily food intake increased by a factor of 1.52 compared to the control group (Figure 1A).

**Table 1. KEGG pathway enrichment of DEGs under acute heat stress**

KEGG Pathway	-LOG <sub>10</sub> (FDR)			DEGs		
	3 h	6 h	12 h	3 h	6 h	12 h
Antigen processing and presentation	4.89	2.80	2.24	CTSL, HSP70, HSP90A	CTSL, HSP70, HSP90A	CTSL, HSP70, HSP90A
Longevity regulating pathway - multiple species	4.57	2.80	2.02	HSP70, CRYAB	HSP70, CRYAB	HSP70, CRYAB
Prion diseases	4.06	ns	1.70	HSP70, STIP1	0	HSP70, STIP1
Legionellosis	3.76	ns	1.53	SdhA, HSP70	0	SdhA, HSP70
Protein processing in endoplasmic reticulum	3.76	1.73	1.40	HSP70, HSP90A, CRYAB, BAG2	HSP70, HSP90A, CRYAB	HSP70, HSP90A, CRYAB, FBXO2
Measles	2.51	ns	ns	HSP70	0	0
Estrogen signaling pathway	2.51	ns	ns	HSP70, HSP90A	0	0
Toxoplasmosis	2.13	ns	ns	HSP70	0	0
Influenza A	1.75	ns	ns	trypsin, HSP70	0	0
Pancreatic secretion	1.61	ns	ns	amyA, trypsin, PNLIP	0	0
Caffeine metabolism	1.61	ns	ns	xdh, uaZ	0	0
Starch and sucrose metabolism	1.59	ns	ns	amyA, malZ	0	0
Steroid hormone biosynthesis	1.56	ns	ns	UGT, CYP3A	0	0
Chemical carcinogenesis	1.52	ns	ns	UGT, CCBL, CYP3A	0	0
Quorum sensing	ns	ns	1.70	0	0	chitinase, GAD

The number of offspring per female was reduced to only 11.6% of the control group (Figures 1B and 1C). The successful parasitism rate witnessed a significant decrease, and their lifespan was drastically reduced by 40% (Figures 1D–1I).

To investigate the impact of heat stress on gene expression and adaptability in the context of aging, as well as to elucidate the mechanisms through which parasitoid wasps modulate gene expression to cope with elevated temperatures, we conducted transcriptome sequencing at various age stages of the adult parasitoid wasps. A total of 1,567,502,192 clean reads were obtained from 36 samples (Table S1). The PCA and cluster analyses revealed two distinct gene expression patterns in response to heat stress: an acute response within the first 12 h, and a chronic response after 5 days (Figures 1J and 1K). Chronic heat stress led to larger gene expression alterations than acute heat stress. We identified 29 up-regulated and 24 down-regulated genes, mainly HSPs, as differentially expressed under acute heat stress. Meanwhile, chronic heat stress resulted in the identification of 323 up-regulated and 354 down-regulated genes, including numerous transcription factors (TFs) (Figure 1L). Top GO terms for up-regulated differentially expressed genes (DEGs) were enriched in peptide activity, while down-regulated DEGs were enriched in binding (Figures 1M and 1N). DEGs were significantly enriched in signaling pathways including “longevity regulating pathway-multiple species,” and “Foxo signaling pathway” (Table 1; Figure 1O). By cross-referencing DEGs with evolutionarily conserved lifespan-related genes,<sup>24</sup> we found that 135 DEGs predictably operate in aging (Table S2).

We employed network analysis to explore the complex interplay between gene expression, environmental temperature, and age. In the construction of the co-expression network, highly related genes were clustered together and assigned distinct colors, yielding 36 color modules (Figure S1A). The blue and turquoise modules, as indicated by the red squares, had more co-expression clustering than the yellow squares (Figure S1B). To examine the association with traits, which included temperature groups and age, the correlation coefficient between traits and the first principal component of the module, i.e., module eigengene (ME), was calculated. Six candidate modules were significantly correlated with temperature and age ( $p < 0.05$ , Figure 2A). Five modules, blue, brown, pink, purple, and yellow modules, were positively correlated with heat stress. There was a significant correlation between age and the turquoise, brown, and purple modules (Figure 2A). Cluster analysis among the modules revealed that the blue and brown modules clustered together, as did the purple and pink modules, while the yellow and turquoise modules were distinct from the others (Figure S1A). The best hub gene of each candidate module was determined, and the one with the highest connectivity in the blue module was named *Xap5 Heat Stress Regulator (XHSR)* (Table 2).

We calculated gene significance (GS) to evaluate the genes’ relevance to group or age categories and module membership (MM) to measure the extent of association between genes and modules. Pearson correlation coefficients between GS and MM were obtained for six modules. Notably, the scatterplot of genes in the blue module presented a linear trend that closely approximated a slope of 1, suggesting a strong positive correlation between GS and MM ( $\text{cor}(\text{GS vs. MM}) = 0.7, p < 0.05$ , Figure 2B). This indicates a strong relationship between genes in the blue module and both the trait and the module itself. Likewise, the correlation between GS and MM for the brown, yellow, and purple modules reached a significant correlation (Figures 2C–2G). Since the brown and purple modules were strongly connected with age traits, genes in these two modules may be linked to the age effect of the heat treatment. This analysis solidly supports the blue module as a highly reliable representation of the transcriptional signatures induced by heat stress.

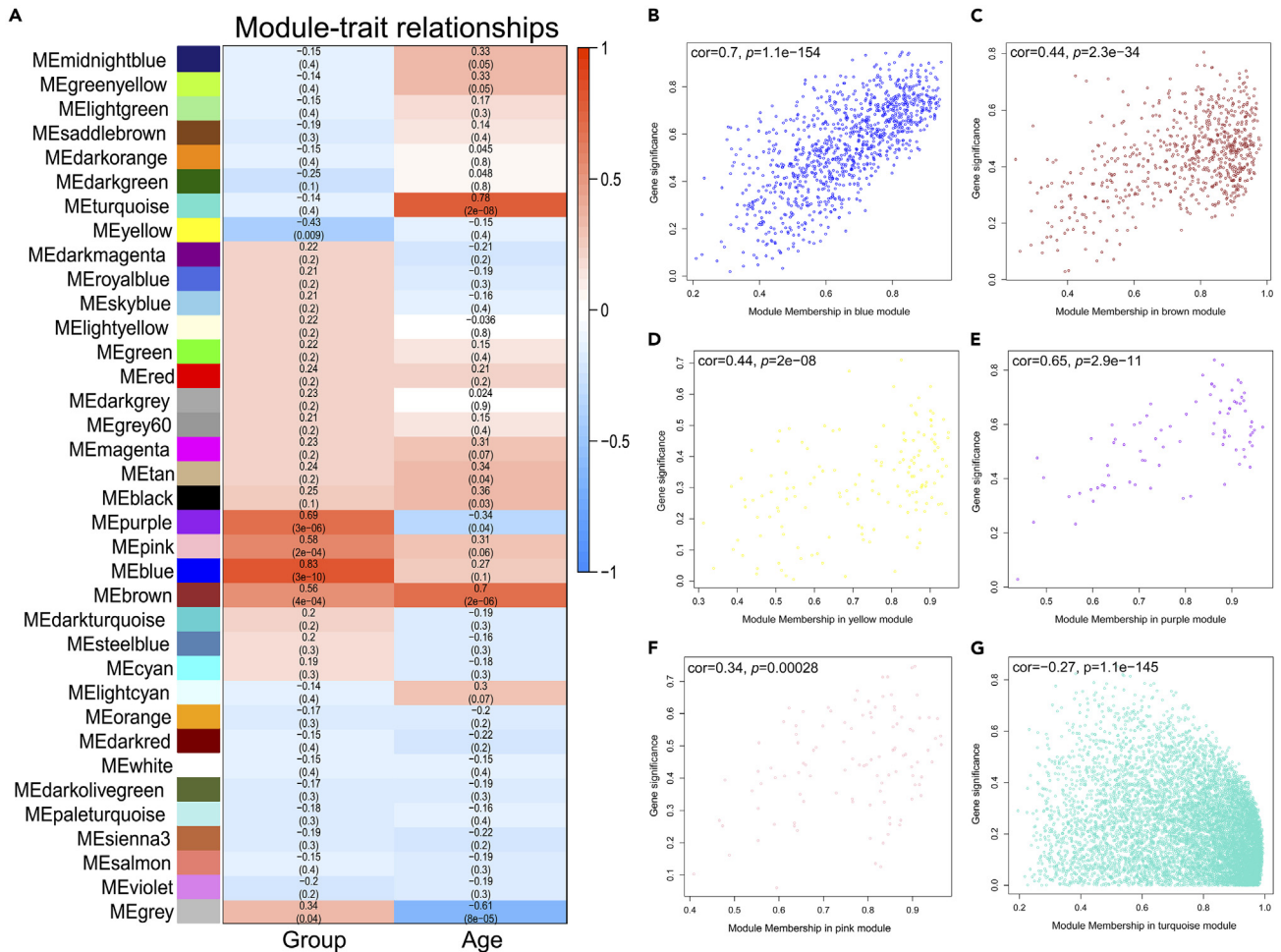


**Figure 2. Weighted gene co-expression network analysis**

(A) Heatmap of module-trait correlations. Each row is a module eigengene (ME). The first column represented different groups. The 25°C group was set as 0, and the 35°C group was set as 1. The second column represented different ages of wasps, from 3 h to 15 days. The correlation coefficient and p value of MEs with traits were marked in each cell, where p values were indicated in parentheses. Blue indicates negative correlation ( $\sim -1$ ) and red indicates positive correlation ( $\sim +1$ ) between the ME and the trait; (B–G) Scatterplot of correlations between GS and MM of candidate modules. Each point indicates a module member (i.e., gene) assigned to each module.

To further explore the attributes of the blue module, we utilized Cytoscape for network visualization, employing a weight threshold of  $>0.2$ , resulting in the identification of 113 core members (Figure 3A). The network is naturally divided into two subgroups, each with a central gene of the highest connectivity: *XHSR* and *PpPPP6A*. *XHSR* had previously been determined as the best hub gene within the blue module. Genes were ranked based on their Maximal Clique Centrality (MCC) score and color-coded, with the top 20 genes predominantly up-regulated (Table S3).<sup>25</sup> Expression patterns of top adjacency genes indicated an age-related increase in  $\log_2$ FoldChange values (Figure 3B). The *XHSR* gene maintained elevated expression levels in the chronic heat stress period, and its expression gradually increased. The fold change

**Table 2. The most highly connected genes in the candidate modules**

Module	Gene ID	Description
blue	PPU15815	<i>XHSR</i> ; Protein FAM50 homolog
brown	PPU08660	RNA polymerase II elongation factor ELL
pink	PPU12978	Venom serine protease BtVSP
purple	PPU16576	60S ribosomal protein L8
yellow	PPU08277	Piwi-like protein Ago3
turquoise	PPU05818	Inner nuclear membrane protein Man1

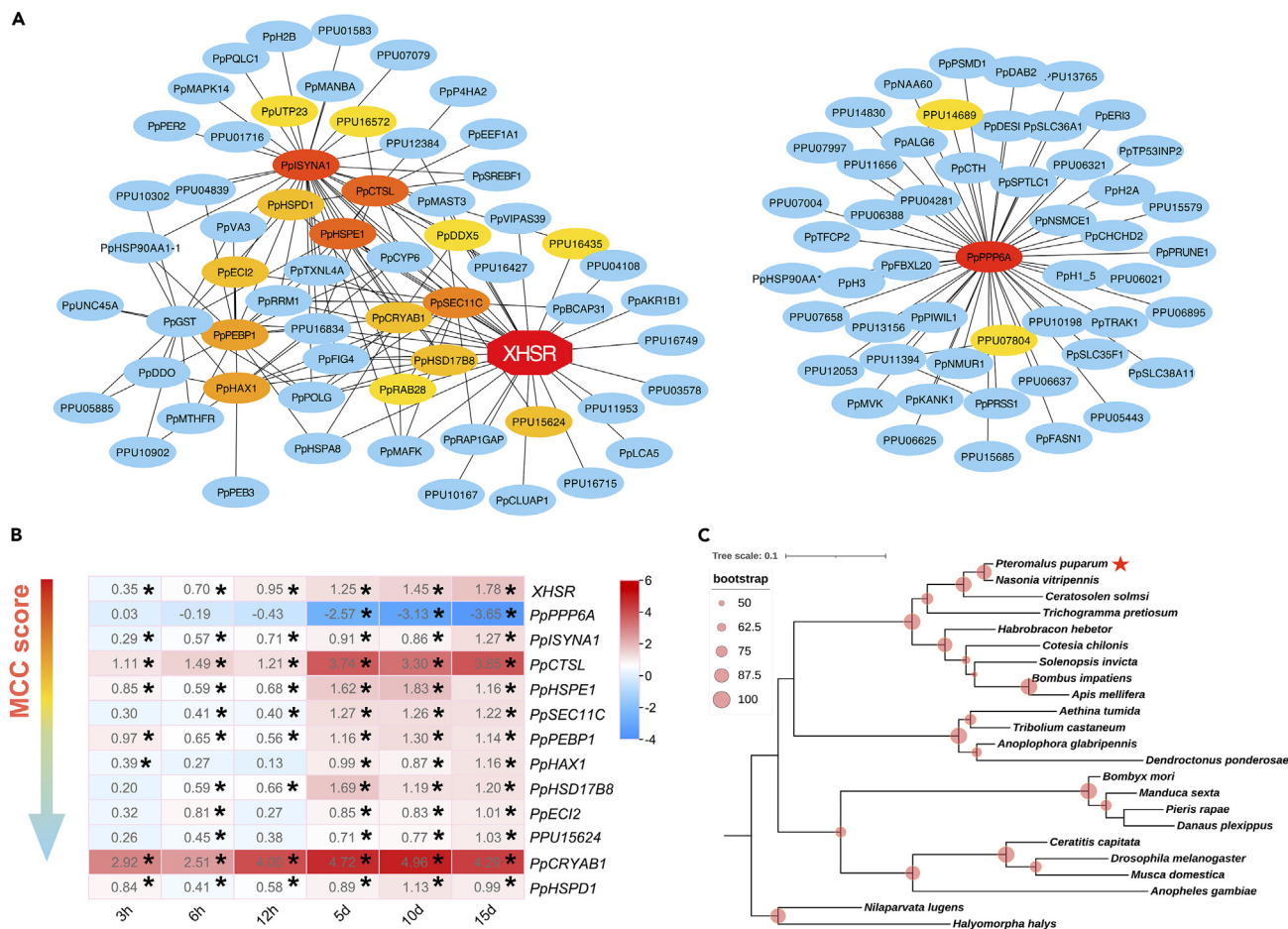


**Figure 3. Regulatory and evolutionary characteristics of blue module candidate hub genes**

(A) The protein-protein interaction (PPI) network for hub genes in the blue module. Genes with weight <0.2 in the network were filtered out and hub genes were predicted. The importance of genes in the network is ranked by MCC and is represented in red, yellow, and blue from highest to lowest; (B) Heatmap of top hub genes ranked by MCC. Each row represented a gene, and each column represented an age. Each cell represented the differential expression of genes in stressed and unstressed conditions for one age group, expressed as  $\log_2$ FoldChange values. \* means  $p < 0.05$ ; (C) Phylogenetic analysis of the homologous genes of XHSR. The maximum-likelihood tree was constructed using IQ-TREE software with 1000 ultrafast bootstrap replicates. XHSR is highlighted with a red star. Circles on the tree branches represent ultrafast bootstrap supports  $\geq 50$ .

values at various ages were 1.3, 1.6, 1.9, 2.4, 2.7, and 3.4 times higher than the baseline (Figure 3B). The KEGG pathway analysis highlighted enrichment of four pathways by six genes, including *PpCTSL*, *PpHSPs*, *PpP38*, and *PpGST* (Figure S2). Integration of  $ME\_blue > 0.8$ ,  $GS\_group > 0.2$ , and  $weight > 0.2$  identified 55 candidate hub genes (Table 3). These core candidates were likely to constitute the regulatory network employed by the parasitoid wasp in response to high temperatures. In order to explore the degree of conservation and potential variations in the critical regulatory genes, we conducted a phylogenetic analysis. This analysis confirmed the conservation of XHSR homologs in Hymenoptera, Coleoptera, Lepidoptera, Diptera, and Hemiptera, including *D. melanogaster*, despite dissimilarity with the XHSR homolog of *P. rapae* (Figure 3C).

Functional information on homologs of core module members was obtained using STRING and ChEA3. The STRING database integrates experimentally validated gene function data from model organisms and generates functional interaction networks *in silico*. Core module memberships of the blue module were inputted into STRING to identify enriched GO terms and pathways (Figure 4A). Using Markov clustering (MCL), 62 *Homo sapiens* homologs of putative hub genes were identified and grouped into eight clusters. Cluster 1 showed intense interactions related to stress response, chaperone function, and acetylation (Figure 4B). Two HSPs and *EEF1A1* were enriched for chaperone mediated autophagy (FDR = 0.0060, Table S4). Cluster 2 included genes involved in fatty-acyl-CoA biosynthesis and the acetyl-CoA metabolic process (Figure 4C). *SREBF1* and *FASN* were enriched by the AMP-activated protein kinase (AMPK) pathway (FDR = 0.0472, Table S5), known for its role in longevity regulation. *KANK1* was identified as an interacting partner of *FAM50A*, the human homolog of XHSR (interaction score >0.3). Gene expression analysis revealed differential expression of HSPs in cluster 1 after acute heat stress, while lipogenesis genes in cluster 2 were not differentially expressed until chronic heat exposure (Figure S3). Key TFs associated with the core module memberships included

**Table 3. Hub genes in the blue module**

Gene ID	Gene Name	Description	kME	GS
PPU15815	XHSR	Protein FAM50 homolog	0.9358	0.8330
PPU04131	PpCRYAB1	Protein lethal (2) essential for life	0.9240	0.8816
PPU01716	PpYNG2	Chromatin modification-related protein	0.9115	0.7003
PPU04112	PpAKR1B1	Aldo-keto reductase AKR2E4	0.9095	0.7602
PPU05064	PpRAB28	Ras-related protein Rab-28	0.9044	0.8286
PPU16943	PpSEC11C	Signal peptidase complex catalytic subunit	0.9030	0.7666
PPU00892	PpPER2	Period circadian protein 2	0.8944	0.7966
PPU04336	PpCHCHD2	Coiled-coil-helix-coiled-coil-helix domain-containing protein 2	0.8942	0.7030
PPU09664	PpCYP6	Probable cytochrome P450 6a14	0.8903	0.7697
PPU08466	PpH2B	Histone H2B	0.8891	0.7451
PPU10167	PPU10167	Protein singed wings 2	0.8833	0.8245
PPU07654	PpEEF1A1	Elongation factor 1-alpha	0.8812	0.6521
PPU15477	PpISYNA1	Inositol-3-phosphate synthase 1-A	0.8799	0.7611
PPU16233	PpHSPE1	10 kda heat shock protein, mitochondrial	0.8782	0.8719
PPU06466	PpPSMD1	26S proteasome non-atpase regulatory subunit 1	-0.8763	-0.7653
PPU03831	PpHSPA8	Heat shock 70 kda protein cognate 4	0.8759	0.8579
PPU00866	PpCTSL	Cathepsin L	0.8752	0.6994
PPU11226	PpHSD17B8	Estradiol 17-beta-dehydrogenase 8	0.8706	0.7439
PPU04477	PpLCA5	Lebercilin	0.8638	0.7469
PPU00422	PpPOLG	DNA polymerase gamma 1	0.8613	0.8944
PPU08409	PpSREBF1	Sterol regulatory element-binding protein 1	0.8589	0.7299
PPU16234	PpHSPD1	60 kda heat shock protein, mitochondrial	0.8582	0.8685
PPU07257	PpP4HA2	Prolyl 4-hydroxylase subunit alpha-2	0.8576	0.6892
PPU02108	PpTXNL4A	Thioredoxin-like protein 4A	0.8562	0.8028
PPU15773	PpFIG4	Phosphatidylinositol 3	0.8508	0.7616
PPU03107	PpPRSS1	Trypsin-1	-0.8504	-0.6260
PPU07010	PpUTP23	U3 small nucleolar RNA-associated protein 23	0.8467	0.7283
PPU07079	PPU07079	Cuticle protein 10.9	0.8458	0.7281
PPU05443	PPU05443	Cuticlin-1	0.8457	0.7024
PPU03644	PpRRM1	Ribonucleoside-diphosphate reductase large subunit	0.8438	0.8396
PPU06969	PpVIPAS39	Spermatogenesis-defective protein 39 homolog	0.8407	0.6972
PPU00804	PpHSP90A1-1	Heat shock protein 83	0.8406	0.8710
PPU02432	PpPEBP1	Phosphatidylethanolamine-binding protein homolog F40A3.3	0.8364	0.7970
PPU07658	PPU07658	Actin-binding Rho-activating protein	0.8346	0.7253
PPU12736	PpMAFK	Transcription factor mafk	0.8335	0.8292
PPU03960	PpDESI1	Desumoylating isopeptidase 1	0.8308	0.6305
PPU07935	PPU07935	Protein disabled	0.8268	0.6469
PPU15624	PPU15624	Uncharacterized protein CG1161	0.8255	0.7972
PPU13156	PPU13156	Protein FAM151A	0.8251	0.6285
PPU01583	PPU01583	Cyclic GMP-AMP synthase	0.8235	0.7991
PPU03794	PpDDX5	ATP-dependent RNA helicase p62	0.8228	0.9310

(Continued on next page)

Table 3. Continued

Gene ID	Gene Name	Description	kME	GS
PPU14775	PpCLUAP1	Clusterin-associated protein 1	0.8220	0.8103
PPU08124	PpGST	Glutathione S-transferase 1, isoform C	0.8220	0.7618
PPU06685	PpPPP6A	Serine/threonine-protein phosphatase 6 regulatory ankyrin repeat subunit A	-0.8204	-0.6491
PPU01592	PpPRUNE1	Exopolyphosphatase PRUNE1	0.8139	0.8059
PPU10765	PpHAX1	Myeloid leukemia factor 2	0.8126	0.6594
PPU08531	PpALG6	Dolichyl pyrophosphate Man9GlcNAc2 alpha-1,3-glucosyltransferase	0.8122	0.7335
PPU06370	PpKANK1	KN motif and ankyrin repeat domain-containing protein	0.8092	0.7196
PPU10036	PpPQLC1	PQ-loop repeat-containing protein 1	0.8068	0.6560
PPU10302	PPU10302	Cerebellar degeneration-related protein 2-like	0.8060	0.7467
PPU11519	PpBCAP31	B-cell receptor-associated protein 31	0.8044	0.7427
PPU10709	PpECI2	Enoyl-coa delta isomerase 2, mitochondrial	0.7964	0.7496
PPU10178	PpNMUR1	Pyrokinin-1 receptor	-0.7756	-0.6206
PPU04656	PpPEB3	Ejaculatory bulb-specific protein 3	0.7736	0.7250
PPU11653	PpVA3	Venom allergen 3	0.7706	0.8186

*SREBF1*, *PEBP1*, *HSPs*, *EEF1A1*, and *FASN* (Figure S4A).<sup>26</sup> The TF co-regulatory network of the top 20 TFs indicated an interaction between TFs *JUN* and *SREBF1* (Figure S4B). Similarity-based text mining results supported the functional significance of *PpSREBF1*, *PpHSPs*, *PpEEF1A1*, and *PpFASN*.

### The vital role of *Xap5* heat shock regulator in the genetic regulatory network

A set of genes identified from DEG and WGCNA analyses underwent quantitative real-time PCR (qPCR) validation after heat stress treatment. The overall expression trends were consistent, despite slight differences compared to transcriptome sequencing results (Figure S5). RNA interference (RNAi) experiments targeting the hub gene *XHSR* were performed at 35°C, using a reporter gene, *Luciferase*, as a control. Major biological parameters, including adult lifespan, intake, offspring number, and %DI, were compared between wasps injected with dsLuc and dsXHSR. Wasps injected with dsXHSR showed a significant 69.3% decrease in *XHSR* expression compared with dsLuc ( $p = 0.0322$ , Figure 5A a). Their mean lifespan significantly decreased at both 35°C and 25°C. At 35°C, dsXHSR wasps exhibited a mean lifespan of 7.0 days, about half of the dsLuc control group ( $p < 0.0001$ , Figure 5A b). While under non-stress conditions at 25°C, dsXHSR wasps had a mean lifespan of 19.2 days, significantly shorter than the 40.1 d observed in the dsLuc control group ( $p < 0.0001$ , Figure 5A c). However, no significant changes were observed in food intake and %DI following dsXHSR injection ( $p > 0.05$ , Figure 5A d-e).

We examined the subnetwork of *XHSR* further because the inhibition of *PpPPP6A* expression had no effect on the mean lifespan of the wasps, compared to the control group ( $p = 0.9172$ , Figure 5B a-b). Lifespan analysis was conducted on wasps injected with dsPpCTSL at 35°C, considering the up-regulation of *PpCTSL* and its close relationship to *XHSR*. dsPpCTSL had 66.9% interference efficiency ( $p = 0.0063$ , Figure 5B c), resulting in an average lifespan of 9.4 days, 18% shorter than the dsLuc group ( $p < 0.0001$ , Figure 5B d).

Following dsXHSR treatments, qPCR was performed on genes adjacent to *PpCTSL* in the co-expression network. The expression of 12 genes was significantly changed, with several genes in cluster 1 of the STRING functional network also significantly changed. No significant changes were observed in the genes of cluster 2, except for *PpSREBF1* (Figure 5A f-l). Based on the STRING database, we hypothesized that *PpFASN1* is related to *PpSREBF1*, which was verified by changes in mRNA levels of *PpFASN1* following dsPpSREBF1 injection (Figure 5B e-g). The mRNA levels of *PpHSD17B8*, *PpPER2*, *PpFIG4*, *PpPRUNE1*, and *PpSPTLC1* were likewise significantly reduced, but to a lesser degree (Figure 5B h-m). The mRNA encoding *PpMVK* remained unchanged.

### Functional implications of the *Xap5* heat shock regulator homolog gene knockout in *Drosophila*

Given the observed conservation of *XHSR* across species (Figure 3C), we conducted a knockout experiment on the *XHSR* homolog *CG12259* in *D. melanogaster* using the CRISPR/Cas9 system to investigate the response of the mutant flies to high temperatures. The selection of *D. melanogaster* as our model stemmed from the hypothesis that *XHSR*'s remarkable conservation across diverse species implies its potential pivotal role in regulating thermal responses. A segment of *CG12259* containing the XAP5 domain on the third chromosome was knocked out and replaced with RFP (Figure 6A). Positive mutants were selected and crossed to obtain heterozygotes ( $\Delta CG12259^{+/-}$ ) with an RFP marker on one chromosome and homozygotes ( $\Delta CG12259^{-/-}$ ) with RFP markers on both chromosomes. A pair of primers designed upstream of the 5' homology arm and on the RFP were used to perform diagnostic PCR, with the wild type as a control. This documented that the target region of

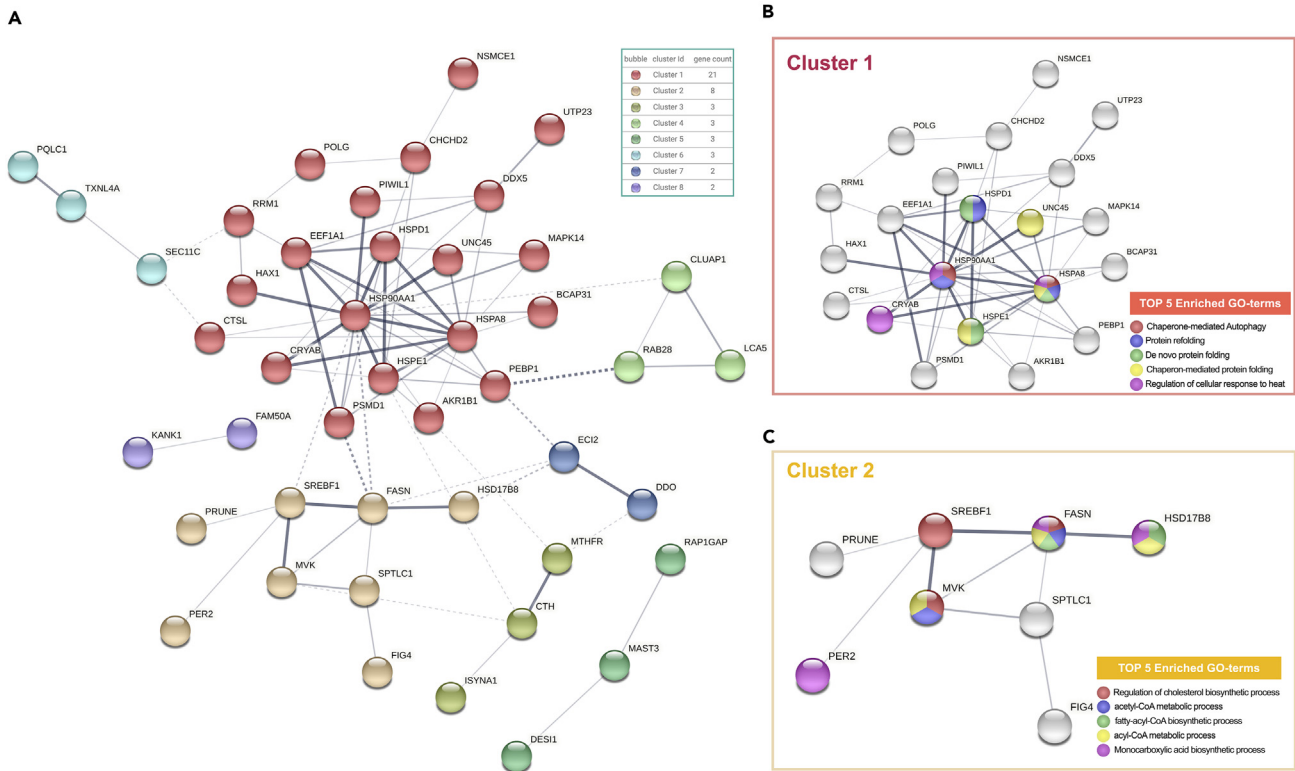


**Figure 4. Interactions between human homologs of candidate hub genes based on STRING database**

(A) The functional network was constructed from genes with interaction scores >0.3, and disconnected nodes were hidden. Edges indicated both functional and physical protein associations, and their thickness indicated the strength of data support. Inside the node bubbles is a preview of the structure of each gene. Nodes were clustered into 8 clusters using MCL clustering, distinguished by color.

(B and C) Interactions between genes in Clusters 1 and 2. The GO enrichment results for the top 5 biological process genes in which nodes were involved were highlighted.

the *CG12259* locus had been knocked out (Figure 6B). At 35°C, all the flies died within two days, with a one-day survival rate of 66.7% (n = 60) for wild-type flies and 33.3% (n = 60) for  $\Delta CG12259^{-/-}$  flies. At 32°C, the survival rate of mutants was significantly lower compared to wild-type flies. The survival rate of  $\Delta CG12259^{-/-}$  flies was lower than  $\Delta CG12259^{+/-}$  flies (Figure 6C, Log rank test,  $p < 0.0001$ ). The median survival of homozygous individuals was 11 days with a mean lifespan of 10.1 days, while heterozygous individuals had a median survival of 12 days with a mean lifespan of 11.2 days. This demonstrates that *CG12259* knock-out significantly compromised the survival of *Drosophila* under high temperatures (32°C and 35°C). This observation is similar to the effect of *XHSR* knockdown in *P. puparum*, which increased the susceptibility of wasps to high temperatures. These findings suggest that the physiological functions of *XHSR* are conserved across different species and can be extrapolated to other organisms.

## DISCUSSION

Heat stress led to impaired fertility shortened lifespan, and compromised ability for host control in *Pteromalus puparum*. In this study, we delved into the effect of high temperature (35°C) on the gene expression profiles in *Pteromalus puparum*, focusing on the intricate regulatory network orchestrating the transcriptional changes.

We determined the genetic mechanism(s) of how heat stress affects traits by identifying genes involved in the *P. puparum* heat stress response. A rapid and discernible change was observed in gene expression profiles in wasps as early as 6 h, following exposure to elevated temperatures. These changes likely signify the activation of stress response mechanisms and the initiation of adaptive strategies aimed at survival. Notably, the major KEGG enrichment pathways among DEGs, especially longevity regulating pathway and the Foxo signaling pathway, suggest a link between these early gene expression changes and the aging regulation in response to heat stress.<sup>24</sup> WGCNA workflow was applied to simplify the transcript profiles and construct a co-expression network. We identified the blue module as the most closely related to the effects of heat stress and was not correlated to age. The hub genes were identified based on the interrelationships and topological structures of genes within the blue module. The best hub gene in the regulatory network was named *XHSR*. Heat stress induced the expression of *XHSR*, and the induction increased with the age of the wasps, while they were continuously exposed to high temperatures. *XHSR* encodes an XAP5-domain protein, the function of which is unknown.

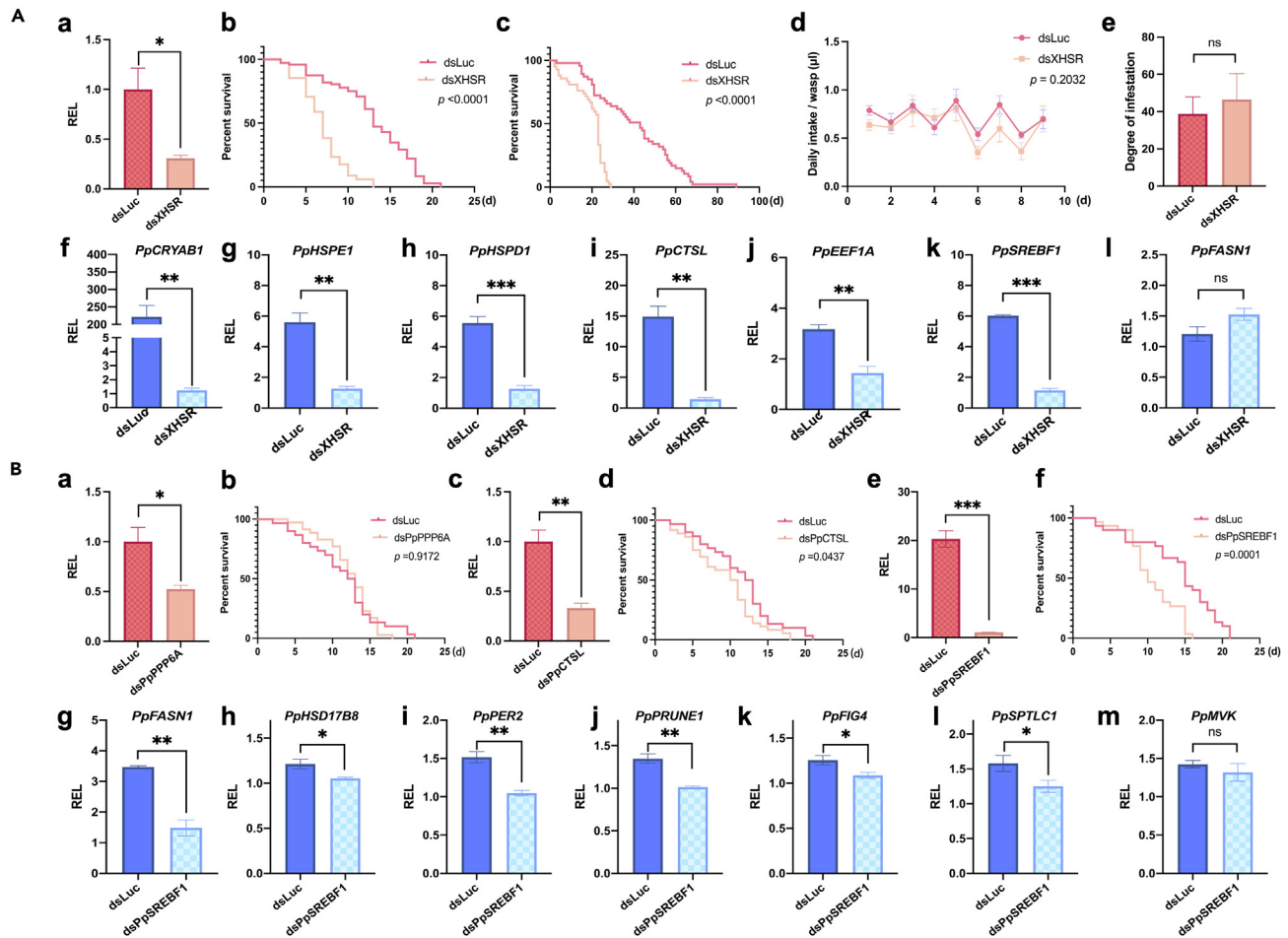


**Figure 5. Effects of RNAi-mediated knock-down of hub genes on wasp fitness and gene expression**

(A) Effects of down-regulation of XHSR expressions by RNAi on regulatory networks and fitness of wasps.

Means  $\pm$  SEM. \* means  $p < 0.05$ , \*\* means  $p < 0.01$ , \*\*\* means  $p < 0.0001$ , ns means  $p > 0.05$ .

(a) Changes in the relative expression levels (REL) of XHSR after injection of dsXHSR; (b) Survival and lifespan of wasps after injection of dsXHSR at 35°C; (c) Survival and lifespan of wasps after injection of dsXHSR at 25°C; (d) Daily food intake per wasp after injection of dsXHSR and dsLuc at 35°C; (e) Degree of parasitism after injection of dsXHSR and dsLuc at 35°C; (f-l) Changes in the REL of other candidate hub genes after injection of dsXHSR. f: *PpCRYAB1*; g: *PpHSPE1*; h: *PpHSPD1*; i: *PpCTSL*; j: *PpEEF1A*; k: *PpSREBF1*; l: *PpFASN1*.

(B) Effects of down-regulation of expression levels of three candidate hub genes by RNAi on wasps' lifespan and regulatory networks. Means  $\pm$  SEM. \* means  $p < 0.05$ , \*\* means  $p < 0.01$ , \*\*\* means  $p < 0.0001$ , ns means  $p > 0.05$ . (a) Changes in the REL of *PpPPP6A* after injection of dsPpPPP6A; (b) Survival and lifespan of wasps after injection of dsPpPPP6A at 35°C; (c) Changes in the REL of *PpCTSL* after injection of dsPpCTSL; (d) Survival and lifespan of wasps after injection of dsPpCTSL at 35°C; (e) Changes in the REL of *PpSREBF1* after injection of dsPpSREBF1; (f) Survival and lifespan of wasps after injection of dsPpSREBF1 at 35°C; (g-m) Changes in the REL of candidate hub genes after injection of dsPpSREBF1. g: *PpFASN1*; h: *PpHSD17B8*; i: *PpPER2*; j: *PpPRUNE1*; k: *PpFIG4*; l: *PpSPTLC1*; m: *PpMVK*.

The functional STRING network exhibited the strength of interactions between human homologs of candidate hub genes. These genes primarily formed two distinct clusters, in which one contained HSPs involving protein folding and the other contained proteins relating to fatty acid metabolism. Based on the STRING database, there is no evidence suggesting that *FAM50A*, the human ortholog of XHSR, is directly involved in the regulation of cellular responses to heat stress or lipogenesis. The distinct cluster characterized by the presence of HSPs within the network aligns with previous studies conducted in other organisms, where experiments have consistently highlighted the induction of HSPs, in particular HSP70 and HSP90 under high temperature conditions.<sup>27</sup> HSP70 facilitates cellular processes through substrate regulation for unfolding, disaggregation, refolding, or degradation.<sup>28</sup> HSP90 plays a role in signal integration and substrate targeting for proteolysis, primarily acting during the later stages of substrate folding, which are critical for cellular signaling and development.<sup>29</sup> In addition, our findings suggest a critical role for CRYAB in the heat stress response. CRYAB is a small heat shock protein that modulates cellular processes related to survival and recovery during stress.<sup>30,31</sup> The induction of CRYABs by *Foxo* and *HSF* contributes to the lifespan extension of *Caenorhabditis elegans*.<sup>32</sup>

The function of hub genes was verified by assessing survival and lifespan changes alongside changes in mRNA levels of downstream genes following knockdown or knockout of selected genes. Suppression of XHSR led to a substantial reduction in wasp lifespan, thus documenting

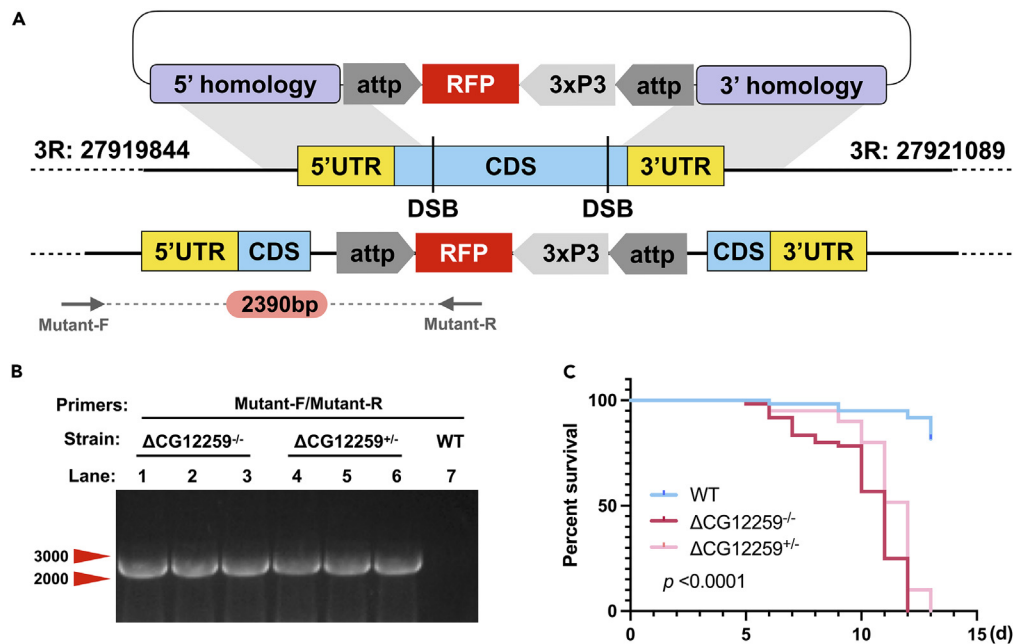


**Figure 6. Knock-out of *Drosophila* XHSR homolog CG12259 using CRISPR/Cas9 system, and the survival of mutants at 32°C**

(A) Schematic representation of the specific recognition of the CG12259 locus, causing double-strand breaks (DSBs), knock out, and replacement of the red fluorescent protein (RFP). A pair of primers for diagnostic PCR was designed upstream of the 5' homology arm on the locus and on the RFP, respectively. The PCR product is 2390bp in length.

(B) Diagnostic PCR using a primer set (arrows in A) in homozygous ( $\Delta$ CG12259<sup>-/-</sup>), heterozygous ( $\Delta$ CG12259<sup>+/-</sup>) and wild-type (WT) individuals.

(C) Survival of homozygous, heterozygous and wild-type female flies at 32°C.

the positive role of XHSR in resistance to heat stress. Furthermore, the reduced lifespan of dsXHSR wasps in normal conditions suggests that XHSR has a broader role beyond the heat stress response, encompassing the regulation of longevity and highlighting its significance in multiple biological processes. While hub genes belonging to cluster 1 of the functional STRING network generally responded to the suppression of XHSR, those belonging to cluster 2 did not, except for *PpSREBF1*. Genes directly down-regulated by repression of XHSR include several HSPs, including *PpEEF1A*, *PpCTSL*, *PpSREBF1*, and among others. This suggested that XHSR may act as an upstream regulator of these genes and respond to acute heat stress by inducing the transcription of HSPs and other genes in cluster 1. Further examination of the mRNA results of hub genes in cluster 2 after injecting dsPpSREBF1 revealed that four genes were directly regulated by *PpSREBF1*. Pathway enrichment analyses suggested that genes in cluster 2 are involved in lipid metabolisms. Based on the expression patterns of genes in cluster 2 (Figure S3), we inferred that these genes respond to chronic heat stress. Other studies have reported possible relationships between these hub genes and stress responses. Mammalian eukaryotic elongation factor 1A (*EEF1A*) has a thermo-sensing capacity.<sup>33</sup> *PpCTSL* encodes a cysteine protease, cathepsin L, whose homologs exist in diverse organisms. Cathepsins are members of a family of proteases that function to degrade intracellular and endocytosed proteins in the lysosome.<sup>34</sup> Cathepsin L plays a crucial role in the apoptosis of midgut epithelium cells, contributing to the remodeling of the larval midgut during metamorphosis in *Helicoverpa armigera*.<sup>35</sup> *PpSREBF1* encodes a sterol regulatory element binding protein. *SREBFs* are conserved in most organisms and regulate the expression of genes required to maintain cellular lipid homeostasis.<sup>36</sup> In *D. melanogaster*, *SREBF* is regulated by levels of phosphatidylethanolamine rather than cholesterol levels. Its targets include acetyl-CoA synthetase, *ACC*, and *FASN*.<sup>37</sup> Taken together, it is inferred that the hub genes in cluster 1 are mediated by XHSR in response to acute heat stress, whereas the hub genes in cluster 2 respond to chronic heat stress through *PpSREBF1*, which is downstream of XHSR (Figure 7).

Evolutionary analysis revealed high conservation and homology of XHSR with multiple species, including *H. sapiens* and *D. melanogaster*. Studies on the fission yeast *Schizosaccharomyces pombe* suggest that XAP5 functions as a chromatin regulator to suppress the expression of antisense and repeat element transcripts across the genome.<sup>38</sup> *XCT*, an *Arabidopsis* ortholog of XAP5, has been implicated in the control of circadian rhythms, ethylene responses, and small RNA synthesis.<sup>39–41</sup> The CRISPR-mediated knock out of *FAM50A* in human cancer cells resulted in a reduction of cellular fitness.<sup>42</sup> Given the high conservation of XHSR across species, we sought to investigate its functional relevance beyond parasitoid wasps. To accomplish this, we turned to *D. melanogaster*, a widely used insect model organism. Through CRISPR/Cas 9-mediated knockout of the XHSR homolog CG12259 in *Drosophila*, we uncovered a significant increase in susceptibility to heat stress, characterized by a notable rise in mortality at high temperatures and a significantly shortened lifespan. These findings suggest that the function of XHSR is likely to be extrapolated and has a critical role in responding to heat stress in other species as well. In addition to their roles in heat stress response, the functions of XHSR and its homolog CG12259 in insects' development warrant attention. The knockout of CG12259 in *D. melanogaster* resulted in normal eclosion, indicating that this gene is non-essential for larval and pupal development. These findings

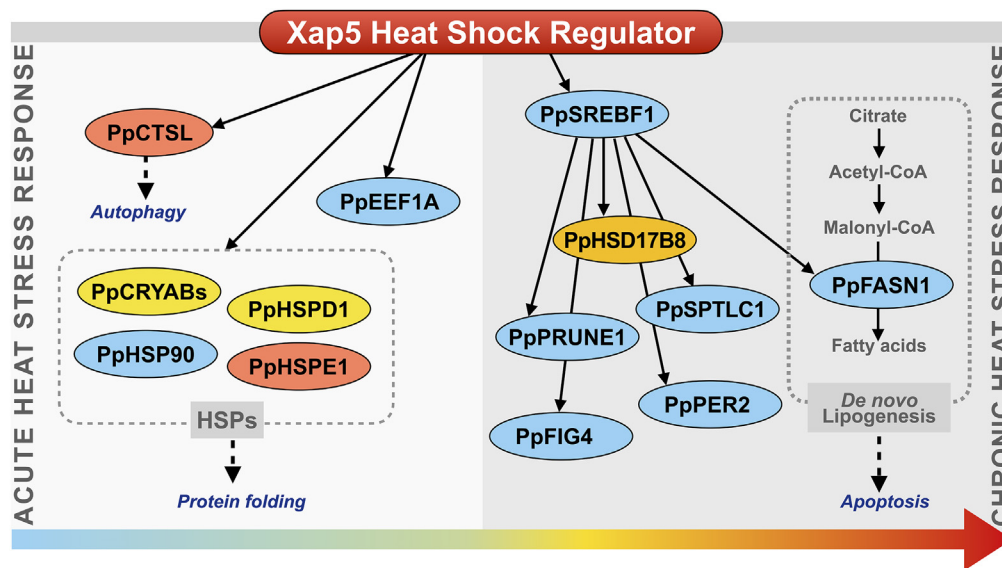


**Figure 7. A model of hub genes in regulatory networks in response to heat stress**

The color of a gene represents its adjacency degree in the regulatory network. Solid arrows indicate gene interactions for which there is experimental evidence, and dotted arrows indicate possible gene functions supported by references.

suggest that *XHSR* and its homolog may exhibit distinct developmental stage-specific functions, with their primary significance emerging in response to heat stress.

The data presented here document the influence of heat stress (35°C) on *P. puparum*, at the physiological and molecular levels. Exposure to 35°C led to decreased longevity and the number of offspring. *P. puparum* is a highly effective biological control agent in agriculture, and, importantly, the 35°C treatment also led to reduced parasitoid efficacy, seen as mortality of pest hosts. Our data indicate that the novel hub gene *XHSR* functions in heat stress response by inducing HSPs and genes involved in lipogenesis. CRISPR/Cas9-mediated knockout of the *XHSR* homolog in *Drosophila* indicates that the function of this gene in heat resistance may be conserved across species. It is not unusual for temperatures in some parts of China to exceed 35°C in the summer and as global temperatures increase, 35°C and higher temperatures will become common. Elevated temperatures produce asymmetry in responses in the host-parasitoid systems. In warmer growing conditions, the pest management efficacy of *P. puparum* and other parasitoid biological control agents can be reasonably expected to decline. Such an effect would have serious negative implications for global food security because many producers are likely to shift their pest control strategies toward increased use of chemical pest control agents. Higher global temperatures may lead to in long-term environmental stewardship. In this context, this study provides new insights into the mechanisms of heat tolerance in insects, including parasitoid wasps, and identifies new candidate genes for improving insect heat resistance for genetic engineering applications.

### Limitations of the study

This study, while informative, has inherent limitations. The experiments were performed in controlled laboratory conditions, which may not fully mirror the complexity of real-world environmental stressors. Our findings, while consistent, were based on laboratory settings, and the translation to natural ecosystems warrants careful consideration. In addition, all experiments exclusively involved female parasitoid wasps. While this gender-specific focus aligns with the greater significance of female parasitoids in pest control, it might introduce a limitation to the applicability of our results across diverse contexts. Further research is required to assess broader ecological applicability and validate findings across diverse species and environments.

### STAR★METHODS

Detailed methods are provided in the online version of this paper and include the following:

- KEY RESOURCES TABLE
- RESOURCE AVAILABILITY
  - Lead contact
  - Materials availability
  - Data and code availability
- EXPERIMENTAL MODEL AND STUDY PARTICIPANT DETAILS
- METHOD DETAILS
  - Insect rearing

- Determination of the lifespan of wasps and fruit flies
- Measurement and statistical analysis of physiological data
- RNA sequencing
- Differential expressed gene analysis
- Weighted gene co-expression network analysis (WGCNA)
- Phylogenetic analysis
- STRING functional associated network and ChEA3 analysis
- RNAi and qPCR analysis
- CRISPR-Cas mutagenesis
- **QUANTIFICATION AND STATISTICAL ANALYSIS**

## SUPPLEMENTAL INFORMATION

Supplemental information can be found online at <https://doi.org/10.1016/j.isci.2023.108622>.

## ACKNOWLEDGMENTS

It was supported by the USDA/Agricultural Research Service. The mention of trade names or commercial products in this article is solely for the purpose of providing specific information and does not imply a recommendation or endorsement by the U.S. Department of Agriculture. All programs and services of the U.S. Department of Agriculture are offered on a nondiscriminatory basis without regard to race, color, national origin, religion, sex, age, marital status, or handicap.

Funding: National Key R&D Program of China (2022YFD1401102), the Program of National Natural Science Foundation of China (32072480), the Key Program of National Natural Science Foundation of China (31830074), Zhejiang Provincial Natural Science Foundation of China (LTGN23C140001), the Fundamental Research Funds for the Central Universities (2021FZZX001-31).

## AUTHOR CONTRIBUTIONS

Conceptualization: SJX, GYY, and QF.  
 Methodology: SJX, XHY, and YY.  
 Investigation: SJX, KLY, and HWL.  
 Visualization: SJX and SX.  
 Supervision: GYY, QF, DS, and QSS.  
 Writing—original draft: SJX and DS.  
 Writing—review & editing: GYY, DS, and QSS.

## DECLARATION OF INTERESTS

Authors declare that they have no competing interests.

Received: September 25, 2023

Revised: October 22, 2023

Accepted: November 30, 2023

Published: December 3, 2023

## REFERENCES

1. Minoli, S., Jägermeyr, J., Asseng, S., Urfels, A., and Müller, C. (2022). Global crop yields can be lifted by timely adaptation of growing periods to climate change. *Nat. Commun.* **13**, 7079.
2. Shi, H., Tian, H., Lange, S., Yang, J., Pan, S., Fu, B., and Reyer, C.P.O. (2021). Terrestrial biodiversity threatened by increasing global aridity velocity under high-level warming. *Proc. Natl. Acad. Sci. USA* **118**, e2015552118.
3. Frölicher, T.L., Fischer, E.M., and Gruber, N. (2018). Marine heatwaves under global warming. *Nature* **560**, 360–364.
4. Woolway, R.I., Jennings, E., Shatwell, T., Golub, M., Pierson, D.C., and Maberly, S.C. (2021). Lake heatwaves under climate change. *Nature* **589**, 402–407.
5. Paaijmans, K.P., Heinig, R.L., Seliga, R.A., Blanford, J.I., Blanford, S., Murdock, C.C., and Thomas, M.B. (2013). Temperature variation makes ectotherms more sensitive to climate change. *Global Change Biol.* **19**, 2373–2380.
6. Sánchez-Guillén, R.A., Córdoba-Aguilar, A., Hansson, B., Ott, J., and Wellenreuther, M. (2016). Evolutionary consequences of climate-induced range shifts in insects. *Biol. Rev. Camb. Phil. Soc.* **91**, 1050–1064.
7. Furlong, M.J., and Zalucki, M.P. (2017). Climate change and biological control: the consequences of increasing temperatures on host-parasitoid interactions. *Curr. Opin. Insect Sci.* **20**, 39–44.
8. Forbes, A.A., Bagley, R.K., Beer, M.A., Hippee, A.C., and Widmayer, H.A. (2018). Quantifying the unquantifiable: why Hymenoptera, not Coleoptera, is the most speciose animal order. *BMC Ecol.* **18**, 21.
9. Takagi, M. (1986). The reproductive strategy of the gregarious parasitoid, *Pteromalus puparum* (Hymenoptera, Pteromalidae). 2. host size discrimination and regulation of the number and sex-ratio of progeny in a single host. *Oecologia* **70**, 321–325.
10. Hu, C. (1983). A survey on the parasites of the small white butterfly, *Artogeia rapae* (L.) in China. *Acta Entomol. Sin.* **26**, 287–294.
11. Wang, H., Li, K., Zhu, J.Y., Fang, Q., Ye, G.Y., Wang, H., Li, K., and Zhu, J.Y. (2012). Cloning and expression pattern of heat shock protein genes from the endoparasitoid wasp, *Pteromalus puparum* in response to environmental stresses. *Arch. Insect Biochem. Physiol.* **79**, 247–263.
12. Jeffs, C.T., and Leather, S.R. (2014). Effects of extreme, fluctuating temperature events on

- life history traits of the grain aphid, *Sitobion avenae*. *Entomol. Exp. Appl.* 150, 240–249.
13. Hussain, M., Lin, Y., and Wang, L. (2017). Effect of temperature on longevity of *Diaphorina citri* (Hemiptera: Liviidae) studied by microcalorimeter. *J. Therm. Anal. Calorim.* 127, 1245–1252.
  14. Vabulas, R.M., Raychaudhuri, S., Hayer-Hartl, M., and Hartl, F.U. (2010). Protein folding in the cytoplasm and the heat shock response. *Cold Spring Harbor Perspect. Biol.* 2, a004390.
  15. Farahani, S., Bandani, A.R., Alizadeh, H., Goldansaz, S.H., and Whyard, S. (2020). Differential expression of heat shock proteins and antioxidant enzymes in response to temperature, starvation, and parasitism in the Carob moth larvae, *Ectomyelois ceratoniae* (Lepidoptera: Pyralidae). *PLoS One* 15, e0228104.
  16. González-Tokman, D., Córdoba-Aguilar, A., Dáttilo, W., Lira-Noriega, A., Sánchez-Guillén, R.A., and Villalobos, F. (2020). Insect responses to heat: physiological mechanisms, evolution and ecological implications in a warming world. *Biol. Rev. Camb. Phil. Soc.* 95, 802–821.
  17. Quan, P.Q., Li, M.Z., Wang, G.R., Gu, L.L., and Liu, X.D. (2020). Comparative transcriptome analysis of the rice leaf folder (*Cnaphalocrocis medinalis*) to heat acclimation. *BMC Genom.* 21, 450.
  18. Bai, Y., Quais, M.K., Zhou, W., and Zhu, Z.-R. (2022). Consequences of elevated temperature on the biology, predation, and competitiveness of two mirid predators in the rice ecosystem. *J. Pest. Sci.* 95, 901–916.
  19. Sarup, P., Sørensen, P., and Loeschcke, V. (2014). The long-term effects of a life-prolonging heat treatment on the *Drosophila melanogaster* transcriptome suggest that heat shock proteins extend lifespan. *Exp. Gerontol.* 50, 34–39.
  20. Hoffmann, A.A., Sørensen, J.G., and Loeschcke, V. (2003). Adaptation of *Drosophila* to temperature extremes: bringing together quantitative and molecular approaches. *J. Therm. Biol.* 28, 175–216.
  21. Evgen'Ev, M.B., Garbuz, D.G., and Zatschina, O.G. (2014). Heat Shock Proteins and Whole Body Adaptation to Extreme Environments, 1 Edition (Springer Dordrecht).
  22. Burdina, E.V., Adonyeva, N.V., Karpova, E.K., Rauschenbach, I.Y., Menshanov, P.N., and Gruntenko, N.E. (2019). The effect of mild heat stress of different frequencies on the adaptability of *Drosophila melanogaster* females. *Arch. Insect Biochem. Physiol.* 102, e21619.
  23. Gruntenko, N.E., Karpova, E.K., Babenko, V.N., Vasiliev, G.V., Andreenkova, O.V., Bobrovskikh, M.A., Menshanov, P.N., Babenko, R.O., and Rauschenbach, I.Y. (2021). Fitness analysis and transcriptome profiling following repeated mild heat stress of varying frequency in *Drosophila melanogaster* females. *Biology* 10, 1323.
  24. Xiong, S., Yu, K., Ye, X., Fang, Q., Deng, Y., Xiao, S., Yang, L., Wang, B., Wang, F., Yan, Z., et al. (2020). Genes acting in longevity-related pathways in the endoparasitoid, *Pteromalus puparum*. *Arch. Insect Biochem. Physiol.* 103, e21635.
  25. Chin, C.H., Chen, S.H., Wu, H.H., Ho, C.W., Ko, M.T., and Lin, C.Y. (2014). cytoHubba: identifying hub objects and sub-networks from complex interactome. *BMC Syst. Biol.* 8 (Suppl 4), S11.
  26. Keenan, A.B., Torre, D., Lachmann, A., Leong, A.K., Wojciechowicz, M.L., Utti, V., Jagodnik, K.M., Kropiwnicki, E., Wang, Z., and Ma'ayan, A. (2019). ChEA3: transcription factor enrichment analysis by orthogonal omics integration. *Nucleic Acids Res.* 47, W212–W224.
  27. Liu, J., Yi, J., Wu, H., Zheng, L., and Zhang, G. (2020). Prepupae and pupae transcriptomic characterization of *Trichogramma chilonis*. *Genomics* 112, 1651–1659.
  28. Rosenzweig, R., Nillegoda, N.B., Mayer, M.P., and Bukau, B. (2019). The Hsp70 chaperone network. *Nat. Rev. Mol. Cell Biol.* 20, 665–680.
  29. Saibil, H. (2013). Chaperone machines for protein folding, unfolding and disaggregation. *Nat. Rev. Mol. Cell Biol.* 14, 630–642.
  30. Boelens, W.C. (2014). Cell biological roles of  $\alpha$ B-crystallin. *Prog. Biophys. Mol. Biol.* 115, 3–10.
  31. King, A.M., and MacRae, T.H. (2015). Insect heat shock proteins during stress and diapause. *Annu. Rev. Entomol.* 60, 59–75.
  32. Morley, J.F., and Morimoto, R.I. (2004). Regulation of longevity in *Caenorhabditis elegans* by heat shock factor and molecular chaperones. *Mol. Biol. Cell* 15, 657–664.
  33. Shamovsky, I., Ivannikov, M., Kandel, E.S., Gershon, D., and Nudler, E. (2006). RNA-mediated response to heat shock in mammalian cells. *Nature* 440, 556–560.
  34. Dana, D., and Pathak, S.K. (2020). A review of small molecule inhibitors and functional probes of Human Cathepsin L. *Molecules* 25, 698.
  35. Yang, C., Lin, X.-W., and Xu, W.-H. (2017). Cathepsin L participates in the remodeling of the midgut through dissociation of midgut cells and activation of apoptosis via caspase-1. *Insect Biochem. Mol. Biol.* 82, 21–30.
  36. Jeon, T.I., and Osborne, T.F. (2012). SREBPs: metabolic integrators in physiology and metabolism. *Trends Endocrinol. Metabol.* 23, 65–72.
  37. Majerowicz, D., and Gondim, K.C. (2013). Insect Lipid Metabolism: Insights into Gene Expression Regulation, 1 Edition (Nova Science Publishers).
  38. Anver, S., Roguev, A., Zofall, M., Krogan, N.J., Grewal, S.I.S., and Harmer, S.L. (2014). Yeast X-chromosome-associated protein 5 (Xap5) functions with H2A.Z to suppress aberrant transcripts. *EMBO Rep.* 15, 894–902.
  39. Martin-Tryon, E.L., and Harmer, S.L. (2008). XAP5 CIRCADIAN TIMEKEEPER coordinates light signals for proper timing of photomorphogenesis and the circadian clock in *Arabidopsis*. *Plant Cell* 20, 1244–1259.
  40. Ellison, C.T., Vandenbussche, F., Van Der Straeten, D., and Harmer, S.L. (2011). XAP5 CIRCADIAN TIMEKEEPER regulates ethylene responses in aerial tissues of *Arabidopsis*. *Plant Physiol.* 155, 988–999.
  41. Fang, X., Shi, Y., Lu, X., Chen, Z., and Qi, Y. (2015). CMA33/XCT regulates small RNA production through modulating the transcription of Dicer-like genes in *Arabidopsis*. *Mol. Plant* 8, 1227–1236.
  42. Thompson, N.A., Ranzani, M., van der Weyden, L., Iyer, V., Offord, V., Droop, A., Behan, F., Gonçalves, E., Speak, A., Iorio, F., et al. (2021). Combinatorial CRISPR screen identifies fitness effects of gene paralogues. *Nat. Commun.* 12, 1302.
  43. Li, B., and Dewey, C.N. (2011). RSEM: accurate transcript quantification from RNA-Seq data with or without a reference genome. *BMC Bioinf.* 12, 323.
  44. Langfelder, P., and Horvath, S. (2008). WGCNA: an R package for weighted correlation network analysis. *BMC Bioinf.* 9, 559.
  45. Nguyen, L.T., Schmidt, H.A., von Haeseler, A., and Minh, B.Q. (2015). IQ-TREE: a fast and effective stochastic algorithm for estimating maximum-likelihood phylogenies. *Mol. Biol. Evol.* 32, 268–274.
  46. Ye, X., Yan, Z., Yang, Y., Xiao, S., Chen, L., Wang, J., Wang, F., Xiong, S., Mei, Y., Wang, F., et al. (2020). A chromosome-level genome assembly of the parasitoid wasp *Pteromalus puparum*. *Mol. Ecol. Resour.* 20, 1384–1402.
  47. Ja, W.W., Carvalho, G.B., Mak, E.M., de la Rosa, N.N., Fang, A.Y., Liang, J.C., Brummel, T., and Benzer, S. (2007). Prandiology of *Drosophila* and the CAFE assay. *Proc. Natl. Acad. Sci. USA* 104, 8253–8256.
  48. Chabert, S., Allemand, R., Poyet, M., Eslin, P., and Gilbert, P. (2012). Ability of European parasitoids (Hymenoptera) to control a new invasive Asiatic pest, *Drosophila suzukii*. *Biol. Control* 63, 40–47.
  49. Martin, M. (2011). Cutadapt removes adapter sequences from high-throughput sequencing reads. *EMBnet. j.* 17, 10–12.
  50. Love, M.I., Huber, W., and Anders, S. (2014). Moderated estimation of fold change and dispersion for RNA-seq data with DESeq2. *Genome Biol.* 15, 550.
  51. Benjamini, Y., and Hochberg, Y. (1995). Controlling the false discovery rate: a practical and powerful approach to multiple testing. *JRSS-B* 57, 289–300.
  52. Shannon, P., Markiel, A., Ozier, O., Baliga, N.S., Wang, J.T., Ramage, D., Amin, N., Schwikowski, B., and Ideker, T. (2003). Cytoscape: a software environment for integrated models of biomolecular interaction networks. *Genome Res.* 13, 2498–2504.
  53. Katoh, K., and Standley, D.M. (2013). MAFFT Multiple Sequence Alignment Software Version 7: Improvements in Performance and Usability. *Mol. Biol. Evol.* 30, 772–780.
  54. Capella-Gutiérrez, S., Silla-Martínez, J.M., and Gabaldón, T. (2009). trimAl: a tool for automated alignment trimming in large-scale phylogenetic analyses. *Bioinformatics* 25, 1972–1973.
  55. Szklarczyk, D., Gable, A.L., Nastou, K.C., Lyon, D., Kirsch, R., Pyysalo, S., Doncheva, N.T., Legeay, M., Fang, T., Bork, P., et al. (2021). The STRING database in 2021: customizable protein-protein networks, and functional characterization of user-uploaded gene/measurement sets. *Nucleic Acids Res.* 49, D605–D612.
  56. Brohée, S., and van Helden, J. (2006). Evaluation of clustering algorithms for protein-protein interaction networks. *BMC Bioinf.* 7, 488.
  57. Livak, K.J., and Schmittgen, T.D. (2001). Analysis of relative gene expression data using real-time quantitative PCR and the 2<sup>-ΔΔCT</sup> Method. *Methods* 25, 402–408.
  58. Labun, K., Montague, T.G., Krause, M., Torres Cleuren, Y.N., Tjeldnes, H., and Valen, E. (2019). CHOPCHOP v3: expanding the CRISPR web toolbox beyond genome editing. *Nucleic Acids Res.* 47, W171–W174.

## STAR★METHODS

### KEY RESOURCES TABLE

REAGENT or RESOURCE	SOURCE	IDENTIFIER
Deposited data		
RNA-seq data	NCBI's GEO database	PRJNA995367 at GEO or SUB13688605 at SRA
Experimental models: Organisms/strains		
<i>Pteromalus puparum</i> : FM(+)	This paper	N/A
<i>Drosophila melanogaster</i> : $y^1w^{1118}$ ; attP40{nos-Cas9}/CyO	UniHuaii Co., Ltd.	CAS-0011(PG2865_01_a)
Oligonucleotides		
Primers for detection of RNAi efficiency, see Table S6	This paper	N/A
Primers for synthesis of dsRNA, see Table S6	This paper	N/A
Primers for qPCR, see Table S6	This paper	N/A
Primers for construction of the recombinant pCFD5 plasmid, see Table S6	This paper	N/A
Primers for diagnostic PCR for positive mutants, see Table S6	This paper	N/A
Recombinant DNA		
Plasmid: CG12259-pCFD5	This paper; Addgene	RRID: Addgene_73914
Plasmid: pBlue-attp-3p3RFP-loxP	This paper	N/A
Software and algorithms		
GraphPad Prism	GraphPad	<a href="https://www.graphpad.com">https://www.graphpad.com</a>
SPSS Statistics	IBM	<a href="https://www.ibm.com/spss">https://www.ibm.com/spss</a>
RSEM	Li and Dewey <sup>43</sup>	<a href="https://github.com/deweylab/RSEM">https://github.com/deweylab/RSEM</a>
DESeq2	Bioconductor	<a href="https://bioconductor.org/packages/release/bioc/html/DESeq2.html">https://bioconductor.org/packages/release/bioc/html/DESeq2.html</a>
WGCNA	Langfelder and Horvath <sup>44</sup>	<a href="https://cran.r-project.org/web/packages/WGCNA/index.html">https://cran.r-project.org/web/packages/WGCNA/index.html</a>
pheatmap	N/A	<a href="https://cran.r-project.org/web/packages/pheatmap/index.html">https://cran.r-project.org/web/packages/pheatmap/index.html</a>
Cytoscape	Cytoscape	<a href="https://cytoscape.org">https://cytoscape.org</a>
OmicShare tools	Gene Denovo	<a href="http://www.omicshare.com/tools">http://www.omicshare.com/tools</a>
IQ-TREE	Nguyen et al. <sup>45</sup>	<a href="http://www.iqtree.org">http://www.iqtree.org</a>

### RESOURCE AVAILABILITY

#### Lead contact

Further information and requests for resources and reagents should be directed to and will be fulfilled by the lead contact, Qi Fang ([fangqi@zju.edu.cn](mailto:fangqi@zju.edu.cn)).

#### Materials availability

This study did not generate new unique reagents.

#### Data and code availability

- RNA-seq data have been deposited at GEO and are publicly available as of the date of publication, under the accession number GEO: PRJNA995367 at NCBI's GEO database or at the NCBI Short Read Archive under submission number SRA: SUB13688605.

- This paper does not report original code.
- For any additional information required to reanalyze the data reported in this paper, please contact the lead author.

## EXPERIMENTAL MODEL AND STUDY PARTICIPANT DETAILS

In this study, we utilized two key experimental models to investigate the impact of elevated temperatures: the parasitoid wasp *Pteromalus puparum* and the fruit fly *Drosophila melanogaster*.

*Pteromalus puparum*, female parasitoid wasps, were subjected to random grouping, with each group consisting of 10 individuals. The wasps were carefully maintained in polystyrene tubes (24 mm D × 95 mm L) to ensure controlled laboratory conditions. The experimental group experienced conditions of 35°C, 60 ± 5% relative humidity, and a 16L:8D photoperiod. In contrast, the control group was maintained at 25°C, 60 ± 5% relative humidity, and the same photoperiod.

In addition to wasps, we integrated *Drosophila melanogaster* as an experimental organism. The fruit flies were housed in polystyrene tubes (24 mm D × 95 mm L). Maintenance conditions for both the CRISPR/Cas9-mediated and wild-type groups were standardized at 35°C, 60 ± 5% relative humidity, and a 16L:8D photoperiod. The G0 generation was established through the injection of plasmids carrying sgRNAs and the Donor plasmid. This resulted in male individuals with the genotype 'yw/Y; attP40{nos-Cas9}/CyO; +/+ ' and female individuals with the genotype 'yw/yw; attP40{nos-Cas9}/CyO; +/+ '. The male G0 (yw/Y; attP40{nos-Cas9}/CyO; +/+) were mated with female flies (yw/yw; +/+; +/+) to produce the G1 offspring, and vice versa with female G0 (yw/yw; attP40{nos-Cas9}/CyO; +/+) being mated with male flies (yw/Y; +/+; +/+). The resulting G1 offspring carried the genotype 'yw/yw; +/CyO or attP40{nos-Cas9}; Marker+ /+'. G1 individuals were mated with those carrying balancer chromosomes (yw/Y; +/+; TM3, Sb/TM6, Tb) to generate the G2 generation. Subsequently, G2 individuals underwent self-mating. The resulting G3 offspring exhibited genotypes, including 'yw/Y; +/+; Marker+/TM3', 'yw/yw; +/+; Marker+/TM3', 'yw/Y; +/+; Marker+/Marker+', and 'yw/yw; +/+; Marker+/Marker+'.

## METHOD DETAILS

### Insect rearing

The *P. puparum* colony used in this study was continuously cultured in the laboratory for over ten generations after initial collection from fields in Hangzhou, China.<sup>46</sup> The wasps were reared in an artificial climate incubator under standard conditions of 25 ± 1°C, 60 ± 5% relative humidity and a 16L:8D photoperiod. After eclosion, adult wasps were mated for three days, then one female wasp and one *P. rapae* pupa were placed in a cylindrical tube for 24 h to breed wasps.

### Determination of the lifespan of wasps and fruit flies

Adult female wasps were promptly collected after eclosion to ensure their virginity and fed on a 10% sucrose solution delivered via a modified capillary feeding method<sup>47</sup> using a capillary tube (1B100F-3; WPI, Sarasota, Florida). Sets of ten female wasps were randomly assigned to groups, with each treatment or control group having three biological replicates. Wasp survival was monitored daily to record life spans.

### Measurement and statistical analysis of physiological data

The daily fluid intake of 10 wasps in a polystyrene tube (24 mm D × 95 mm L) was measured to determine the daily wasp intake. Three biological replicates were measured at 25°C and 35°C, respectively. To measure daily fluid intake, we used multiple capillaries initially filled to the same level. The reduction in liquid level within these capillaries was recorded and used to calculate intake by subtracting the portion attributed to evaporation. Following two days of mating after eclosion, fresh host pupae were provided daily until each wasp died. The counts of *P. rapae* adults (*ri*) and of *P. puparum* (*pi*) were recorded. Apart from successful parasitism, parasitic behaviors such as the injection of venom could lead to death of the butterflies. The degree of infestation (%DI) was introduced as a measure of the proportion of butterflies that died due to parasitization or envenomation, estimated as  $((T - ri) / T) \times 100$ , where *T* is the average number of emergent hosts in the absence of the parasitoid. The rate of successful parasitism (%SP) was determined as  $[pi / (T - ri)] \times 100$ ,<sup>48</sup> representing the probability of an infested host giving rise to an adult wasp. The biological parameters, including food consumption, offspring number, %SP and %DI, were analyzed using the IBM SPSS Statistics for Mac, Version 25.0 (Armonk, NY: IBM Corp). Normality was tested using the Shapiro-Wilk test, and homogeneity of variance was assessed using Levene's test. Mann-Whitney tests were employed for analyzing wasps' food intake and offspring number, while student's *t* tests were performed for %DI and %SP. Survival curves were plotted using the Kaplan-Meier method and differences in lifespan between groups were evaluated by the Log-rank (Mantel-Cox) test, using GraphPad Prism version 9.0.0 for Mac (GraphPad Software, San Diego, California USA, [www.graphpad.com](http://www.graphpad.com)).

### RNA sequencing

Newly-emerged female individuals of similar size were randomly assigned to two groups. One group was reared in 25°C incubators and the other in 35°C incubators to impose heat stress. Samples were collected from both groups after 3 h, 6 h, 12 h, 5 d, 10 d and 15 d of temperature treatments. Based on our gene expression pattern analyses, we categorized the responses to heat stress into two distinct phases: an acute response for the first 3 h, 6 h, and 12 h, and a chronic response for the subsequent 5 d, 10 d, and 15 d. Three replicates were set up for each group, and five female wasps were collected from each replicate (creating 36 samples), treated with TRIzol. The samples were used

for RNA-Seq and subsequent differential expression analysis. The Illumina Truseq™ RNA sample prep Kit was used for library construction. The raw sequencing data were obtained from HiSeq platform. Then the raw data underwent quality control using cutadapt v1.16 to obtain clean reads.<sup>49</sup> The data were spliced based on the Trinity assembly algorithm and combined with the genomic data for subsequent analysis. The two un-filtered paired-end lanes of each sequence run have been deposited as a series, under the accession number PRJNA995367 at NCBI's GEO database or at the NCBI Short Read Archive under submission number SUB13688605.

### Differential expressed gene analysis

Gene expression levels were calculated separately for each treatment and control group using the RSEM software package.<sup>43</sup> Differential gene expression analysis between the two treatments was performed using the R package DESeq2.<sup>50</sup> The  $p$  values were corrected for false discovery rate (FDR) using the Benjamini-Hochberg procedure.<sup>51</sup> The results were expressed as  $q$  values and the fold change of difference was calculated. A gene was considered differential expressed (DEG) if its  $q < 0.05$  and  $\text{abs}(\log_2\text{FoldChange}) > 1$ . Comparison of DEGs was performed between each treatment and control group pair at six time points. Cluster analysis for all genes in the *P. puparum* genome was conducted using the R package pheatmap. Principal component analysis (PCA), volcano map, Venn diagram, Gene Ontology (GO) and KEGG pathways analyses were performed using OmicShare tools (<http://www.omicshare.com/tools>). GO terms and KEGG pathways with  $q < 0.05$  were considered significantly enriched.

### Weighted gene co-expression network analysis (WGCNA)

Weighted gene co-expression network analysis was constructed using the R package WGCNA v1.66.<sup>44</sup> Genes with low expression (FPKM = 0) in all samples were filtered out, resulting in 13,948 genes used for WGCNA. The following parameters were applied: “–network type = unsigned, –soft power = 8, –module identification method = dynamic tree cut, –minimum module size = 30, –merge modules with a high similarity = 0.2”. Default values were used unless specified. The correlation between gene modules and the traits was evaluated. After screening out the target modules, the gene interaction network was visualized using cytoscape 3.8.2 software.<sup>52</sup> CytoHubba was used to identify candidate hub genes within the modules.<sup>25</sup>

### Phylogenetic analysis

All resulting protein sequences were first aligned with MAFFT v7.123b (parameters: –maxiterate 1000) and then trimmed by trimAl v1.4.rev22.<sup>53,54</sup> The best substitution model was determined by the ModelFinder implemented in IQ-TREE v1.6.7 according to Bayesian Information Criterion (BIC).<sup>45</sup> Phylogenetic trees were constructed by IQ-TREE with 1000 ultrafast bootstrap replicates.

### STRING functional associated network and ChEA3 analysis

The core module memberships were entered into the STRING Search tool and a confidence interaction score of 0.3 was applied to maintain functional interactions.<sup>55</sup> The core module memberships were clustered using MCL Clustering.<sup>56</sup> We also predicted TFs that may act downstream of core module memberships using ChEA3.<sup>26</sup>

### RNAi and qPCR analysis

Synthesis of double-strand RNA (dsRNA) targeting hub genes was performed using a MEGAscript® T7 Transcription Kit (Ambion, Austin, TX). Primers were designed on Primer3web (version 4.1.0) and the sequences are shown in Table S6. At least two pairs of specific primers were designed for each tested gene. A dsRNA sequence targeting *Luciferase* was generated as a negative control. The concentration and purity of dsRNA were measured using the NanoDrop spectrophotometer (Thermo Scientific). Microinjection was conducted using the Nanoject III injector (Model #3-000-207, Drummond Scientific Company, Broomall, PA). The RNAi efficiency was assessed by qPCR.

We sampled wasps for qPCR in parallel with the lifespan experiments. cDNA was synthesized using a PrimeScript™ One Step RT-PCR Kit (Takara, Japan). qPCR reactions were carried out using ChamQ™ SYBR qPCRMaster Mix (Without ROX) (Vazyme Biotech Co., Ltd). A 25  $\mu$ l reaction volume containing 10 ng cDNA was used as the template for qPCR. Each sample was analyzed in three biological replicates. A dissociation curve was included from 60–95 °C at the end of each qPCR reaction to verify the specificity of each primer pair. We performed qPCR for the templates with serial dilutions from 10 to 100,000, respectively, and calculated their efficiency values. Appropriate primers were selected for the gene expression profiling. Ribosome RNA (18s) was used as a reference gene. The relative mRNA expression levels were calculated using the  $2^{-\Delta\Delta C_t}$  method.<sup>57</sup> These data were plotted using GraphPad Prism. Relative expression levels of genes were presented as means  $\pm$  SEM and analyzed by two-way ANOVA. Differences were considered significant when  $p < 0.05$ .

### CRISPR-Cas mutagenesis

We used a CRISPR/Cas9 system to knock out *XHSR* homolog *CG12259* gene in *D. melanogaster* with a red fluorescent protein (RFP) inserted. Three guide RNA (gRNA) targets and protospacer-adjacent motifs (PAMs) were assessed *in silico* using CHOPCHOP.<sup>58</sup> A pCFD5 plasmid with three gRNAs inserted was generated to induce double-strand breaks (DSBs) on the target sequence (<http://www.crisprflydesign.org/plasmids/>). A donor plasmid was constructed to provide a template for homologous repair, which contained an RFP transcription unit under the control of the 3xP3 promoter enclosed within two attP recombination sequences, both 5' and 3', flanked by 1 kb sequence upstream and downstream, respectively, of the target site in *CG12259* locus. Transgenic flies were generated by micro-injection of the indicated constructs

into *yw; nos: Cas9/Cyo* stock (UniHuaii Co., Ltd.) using the CRISPR/Cas9 system (Table S7). All surviving G0 flies were crossed to wild-type flies and G1 transformants with red fluorescence were selected under LED illumination (Model: M-IL-FOI 2003, OPLENIC CORP, U.S.A.). The G1 positive flies were crossed to flies carrying the *TM3, sb/TM6B, tb* balancer chromosome, and screened for heterozygous  $\Delta CG12259^{+/-}$ , and then self-crossed to obtain homozygous  $\Delta CG12259^{-/-}$  stocks.

### QUANTIFICATION AND STATISTICAL ANALYSIS

The biological parameters, including food consumption, offspring number, %SP and %DI, were analyzed using the IBM SPSS Statistics for Mac, Version 25.0 (Armonk, NY: IBM Corp). Normality was tested using the Shapiro-Wilk test, and homogeneity of variance was assessed using Levene's test. Mann-Whitney tests were employed for analyzing wasps' food intake and offspring number, while student's *t* tests were performed for %DI and %SP. Survival curves were plotted using the Kaplan-Meier method and differences in lifespan between groups were evaluated by the Log-rank (Mantel-Cox) test, using GraphPad Prism version 9.0.0 for Mac (GraphPad Software, San Diego, California USA, [www.graphpad.com](http://www.graphpad.com)). The results of qPCR were plotted using GraphPad Prism. Relative expression levels of genes were presented as means  $\pm$  SEM and analyzed by two-way ANOVA. Differences were considered significant when  $p < 0.05$ .